24th COBEM - 2017

24th ABCM International Congress of Mechanical Engineering
December 3-8, 2017, Curitiba, PR, Brazil

COBEM-2017-0441
EXPERIMENTAL FLOW-INDUCED MOTIONS OF ARRAY OF FLOATING CYLINDERS WITH CIRCULAR, SQUARE AND DIAMOND SECTIONS

Rodolfo Trentin Gonçalves
The University of Tokyo, Dept. of Ocean Technology, Policy, and Environment, Kashiwa-shi, Chiba, Japan
goncalves@edu.k.u-tokyo.ac.jp

Maria Eduarda Felippe Chame
University of São Paulo, Dept. of Naval Architecture and Ocean Engineering, São Paulo, SP, Brazil
dudafchame@gmail.com

Nicole Hepp Hannes
Federal University of Santa Catarina, Dept. of Mobility Engineering, Joinville, SC, Brazil
nicole@hannes.com

Pedro Paludetto Silva de Paula Lopes
University of São Paulo, Dept. of Naval Architecture and Ocean Engineering, São Paulo, SP, Brazil
lopes.paludetto@gmail.com

Hideyuki Suzuki
The University of Tokyo, Dept. of Systems Innovation, Bunkyo-ku, Tokyo, Japan
suzukih@sys.t.u-tokyo.ac.jp

Shinichiro Hirabayashi
The University of Tokyo, Dept. of Ocean Technology, Policy, and Environment, Kashiwa-shi, Chiba, Japan
hirabayashi@k.u-tokyo.ac.jp

Abstract. *Experiments regarding the FIM - flow-induced motions on an array of three and four floating cylinders with low aspect ratio, $H/L = 1.5$, with the distance between column centers, $S/L = 4$, were carried out in a towing tank. The array of cylinders was elastic supported by a set of linear springs to provide low structural damping on the system. Three different section geometries were tested, namely circular, square and diamond. One current incident angle was tested, as 0 degrees. These configurations of arrays were selected to cover the range of the main offshore multi-column platforms, such as SS - semi-submersible, TLP – tension leg platform and FOWT – floating offshore wind turbine. The aims were understanding from fundamental tests the VIM – vortex-induced motions of the multi-column systems and compare the results of the single column. The range of Reynolds number covered 10,000 < Re < 150,000. For the single cylinders, the amplitude results showed a VIV – vortex-induced vibrations behavior for the single circular cylinder; for the single square cylinder, galloping behavior was observed for 0-degree incidence, and VIV one was observed for 45-degree incidence (diamond cylinder). For the array of four circular cylinders, the amplitude results in the transverse direction showed a VIV behavior for the circular cylinders and galloping was observed for four square cylinders. The amplitude results for the array of four cylinders were very similar to single cylinders for this distance between cylinders. These results are larger than VIM results obtained from a floating system with pontoons. For the array of three cylinders, the amplitude results showed to be larger than the array of four cylinders in high reduced velocities. Results of amplitudes and frequencies in the in-line and transverse directions corroborated for these statements.*

Keywords: *flow-induced motion, vortex-induced vibrations, galloping, array of cylinders, towing tank*

1. INTRODUCTION

Works about fundamental FIV – flow-induced vibrations of low aspect ratio circular cylinders are few in the literature; among which Rahman & Thiagarajan (2013), Gonçalves et al. (2014) and Zhao & Cheng (2014) can be highlighted

concerning studies for low aspect ratio circular cylinders. Moreover, Gonçalves et al. (2015b, 2016) presented results for low aspect ratio square cylinders with 0 and 45-degrees incidence and showed the different behavior for the cylinders with square and circular sections. It was possible to conjecture that the FIV for square cylinders with 0-degree incidence was more similar to the galloping phenomenon. However, for square section cylinder with 45-degree incidence, the behavior was more similar to the VIV phenomenon as in the circular section cylinder case. The same statements can be found in Zhao et al. (2014) for long cylinders with square sections.

The offshore industry demanded the interest in the VIV around cylinders with low aspect ratio, $0.3 < H/L < 6.0$, and small mass ratio, $m^* < 6$. This specific subject was called VIM, see works by Gonçalves *et al*. (2012) and Fujarra *et al*. (2012) for details about VIM, whose motivation has been the higher current velocity incidence on circular offshore platforms, in particular cases of spar, $1.5 < H/L < 6.0$, and monocolumn, $0.2 < H/L < 0.5$.

The VIM has also been studied on the multi-columns platform, such as SS, TLP, and FOWT. Recently, the column section geometry has been considered. For example, the works by Gonçalves *et al.* (2015a) present a comparison between VIM results for circular and square column sections. Other works related to the same research area can be cited such as Liu *et al.* (2016a) and Ramirez & Fernandes (2016), in which the comparison between VIM results for square and diamond section columns were presented. All the works showed that the VIM response is profoundly impacted by the column section geometry as well as by the incidence angle of the current.

Recently, the development of FOWT have been increasing because of the Japanese demand for new clean energy sources, see for example Wang *et al*. (2010) and Liu *et al*. (2016b). In these works, the authors presented the new developments of FOWT and showed that the largest number of designs are multi-columns floaters with three columns. Particularly, the Fukushima project developed FOWT with an array of three columns in a triangle disposition, with circular and square columns, as can be seen in Fig. 1. There are not works in the literature talking about the flow around an array of three cylinders and neither about VIM on these systems. The column section geometry also has been considered for the FOWT designs.


(a)

(b)

Figure 1: Examples of FOWT with three columns in a triangle disposition: (a) Fukushima Mirai Wind Turbine; (b) Fukushima Shimpuu Wind Turbine.

In this context, our aims here are to understand, with fundamental experiments in a towing tank, the FIM around an array of three and four floating cylinders, $m^* = 1$, with the typical value of the aspect ratio of the columns of multi-column platforms, $H/L = 1.5$, and typical distance between column centers $S/L = 4$. Another issue is to compare the results with single column cases.

2. EXPERIMENTAL PROCEDURE

All the experiments were carried out in a towing tank at the UTokyo – University of Tokyo, Hongo, Tokyo, Japan. The dimension of the test section is 85.0m x 3.5m x 2.4m (length x wide x depth), see Fig. 2(a). The maximum velocity of the towing car was around 0.4m/s.


(a)

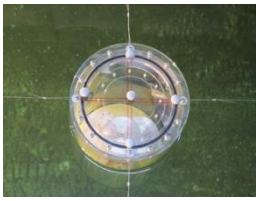
(b)

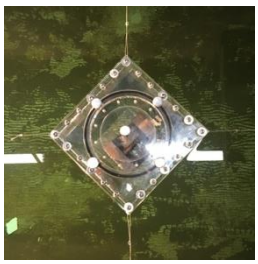
(c)

Figure 2: Illustrative photos of the model tests. (a) Towing tank at Hongo Campus; (b) Circular cylinder; (c) Square cylinder with 45-degree incidence.


(a)

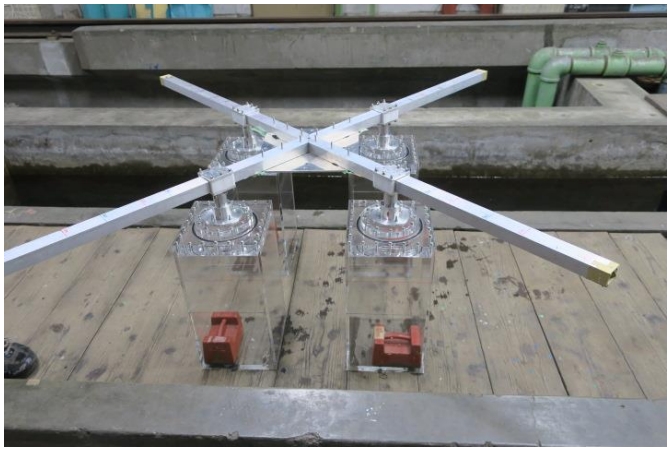
(b)

Figure 3: Illustrative photos of the model tests in the support. (a) Array of four circular cylinders; (b) Array of four square cylinders

Figure 4(a-b) presents a photo of the array of the three diamond cylinders.


(a)


(b)

Figure 4: Illustrative photos of the array of three cylinders (a) Top view, diamond, $S/L = 3$, 90 degrees; (b) Front view, diamond, $S/L = 3$, 90-degree incidence.

The circular column models were made of acrylic with external diameter $D = L$ =250mm (Fig. 2(b)), as well as the square (diamond) column models with face dimension L =220mm (Fig. 2(c)). The cylinders did not present roughness level and may be considered smooth cylinders. Cross bar was designed to support the array of three and four cylinders. The support allowed easy change of column geometry and distance between column centers. The model was elastically supported by a set of 4 horizontal mooring lines. The 6 DOF – degree-of-freedom motions data was acquired along 70m in the towing tank with the sampling frequency of 30Hz using an optical motion capture system. Figure 3(a) presents a photo of the array of the four circular cylinders and Fig. 3(b) presents the array of the four square cylinders.

Three different configurations were tested, namely: circular cylinder, square, and diamond with one angle of the current incidence as 0 degrees. Figure 5 and Fig. 6 show the configurations tested. All the experiments were carried out with the same mooring line and stiffness configuration. Table 1 presents details about the configurations tested.

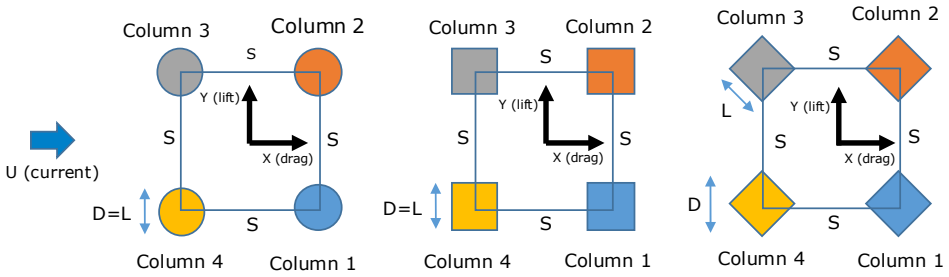

Figure 5: Schematic of the configurations of the array of four cylinders tested, circular, square and diamond for 0-degree incidence

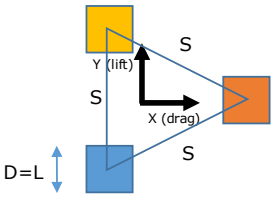

Figure 6: Schematic of the configurations of the array of three cylinders tested, square and 0-degree incidence.

Table 1 – Matrix of conditions carried out for FIV studies of cylinders

Cylinder section geometry	*Current incidence angle [degree]*	*L [mm]*	*D [mm]*	*H/L*	*H/D*	*S/L*	*S/D*	*Re x* 10^{-3}	*Number of columns*
Circular	0	250	250	1.5	1.5	-	-	15 – 100	20
Square	0	220	220	1.5	1.5	-	-	11 – 89	18
Diamond	0	220	311	1.5	1.1	-	-	24 – 150	18
Circular	0	250	250	1.5	1.5	4.0	4.0	15 – 85	15
Square	0	220	220	1.5	1.5	4.0	4.0	10 – 70	20
Diamond	0	220	311	1.5	1.1	4.0	2.8	15 – 90	20
Square	0	220	220	1.5	1.5	4.0	4.0	10 – 75	30
Diamond	0	220	311	1.5	1.1	4.0	2.8	25 – 110	30

3. RESULTS AND DISCUSSION

The FIM response was analyzed through the RMS - root mean square of displacements in the transverse direction and angles of rotation in the case of the yaw motion. Moreover, as commonly found, non-dimensional nominal amplitudes in the transverse direction were calculated as a quotient of the $\sqrt{2}$ times the RMS displacements, A_y, by the face dimension of the column, L. For the RMS angles of yaw, A_{yaw}, no dimensionless presentation was adopted, as usual in the literature.

The characteristic motion periods were calculated for the motions in the transverse direction, T_y. The characteristic motion was defined as the peak of the highest energy level in the PSD - power spectrum density. The results will be presented in the non-dimensional form using the natural period in still water, i.e., T_y/T_{0y}.

The reduced velocity $V_r = UT_{0y}/D$ was defined as a function of the incident current velocity, U, the natural period of the transverse motion in still water, T_{0y}, and the characteristic length of the body section subjected to a vortex shedding, D. In this case, D can be written as a function of the current incidence angle for square columns, to better represent the characteristic length of the column section on the flow, i.e. $D = L(|sin\theta| + |cos\theta|)$, where θ is the current incidence angle. For circular columns cases $D = L$ for all incidence angles.

3.1 Single cylinder

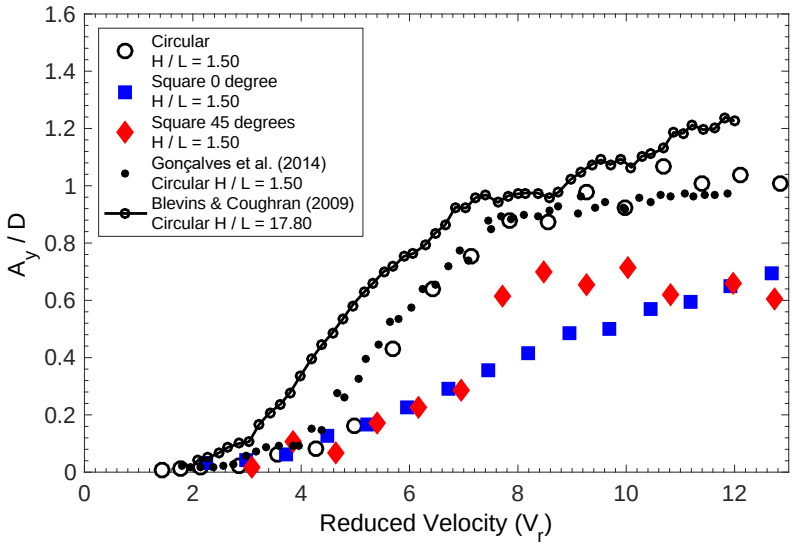

Figure 7: Nondimensional motion amplitude in the transverse direction (A_y/D) as a function of the reduced velocity (V_r) for floating circular, square with 0-degree and 45-degree (diamond) cylinders.

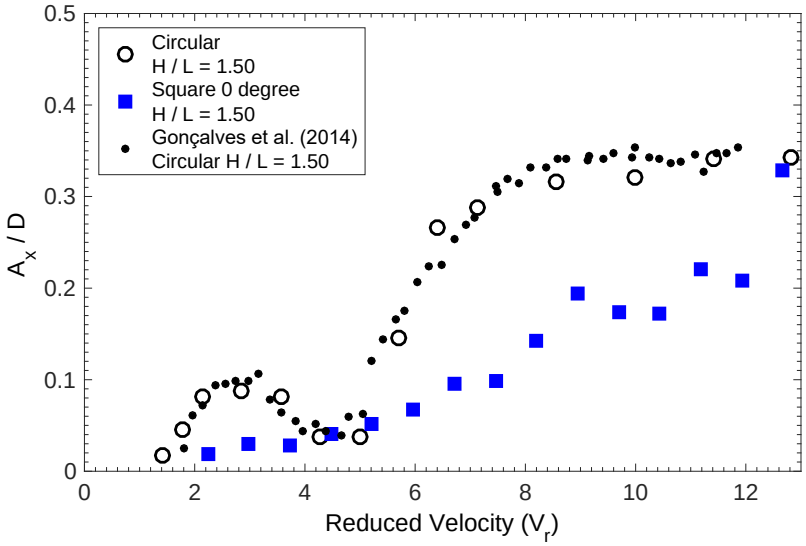

Figure 8: Nondimensional motion amplitude in the transverse direction (A_x/D) as a function of the reduced velocity (V_r) for floating circular, square with 0-degree and 45-degree (diamond) cylinders

Figure 7 presents the results of the A_y/D – nondimensional nominal motion amplitude in the transverse direction as a function of the V_r for the floating circular, square with 0-degree and 45-degree (diamond) cylinders. The results showed that the highest amplitudes occurred for the circular cylinder, and the VIV behavior is the same presented by Gonçalves *et al.* (2014). Moreover, the square cylinder with 0-degree incidence showed a linear increase in the amplitude with the increase in the V_r; this behavior confirms the galloping phenomenon for this cylinder geometry. On the other hand, the square cylinder with 45-degree incidence presented a resonance response for the range $7 < V_r < 11$; that confirms the VIV phenomenon for this cylinder geometry.

Figure 8 presents the results of the A_x/D - nondimensional nominal motion amplitude in the in-line direction as a function of the V_r for the floating circular, square with 0-degree and 45-degree (diamond) cylinders. The results showed the highest amplitudes for the circular cylinder; and in this case, it is possible to verify the VIV in-line resonance for the range $2 < V_r < 4$, as presented in Gonçalves *et al.* (2014). On the other hand, the square cylinder with 0-degree incidence showed a linear increase in the amplitude with the increase in the V_r; this behavior confirms the galloping phenomenon for this cylinder geometry.

3.2 Array of four cylinders

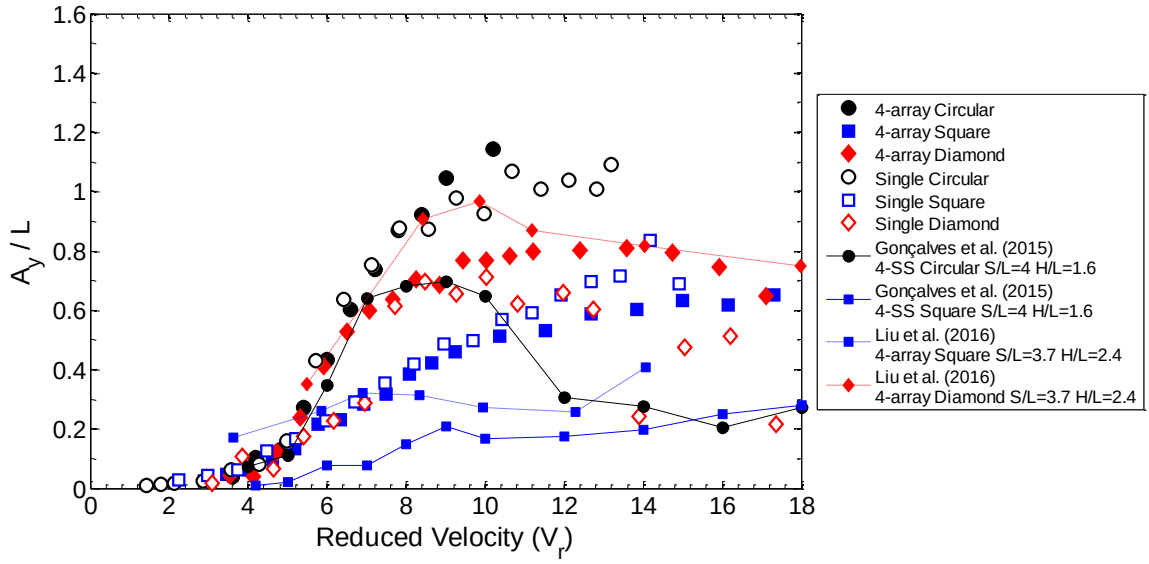

Figure 9: Nondimensional motion amplitude in the transverse direction (A_y/L) as a function of the reduced velocity (V_r) for array of four floating cylinders with circular, square and diamond sections for 0-degree incidence

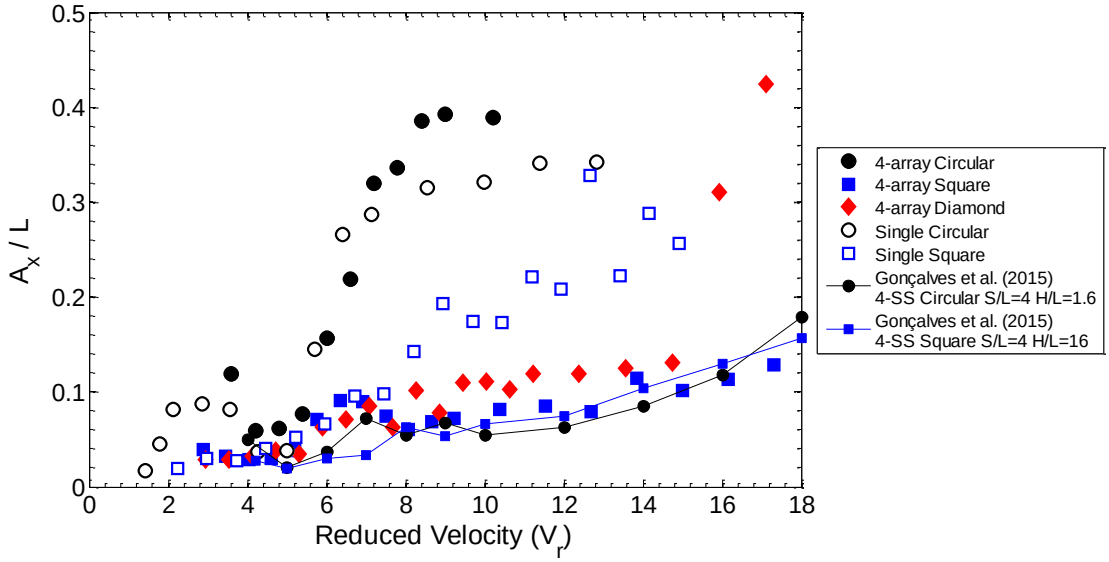

Figure 10: Nondimensional motion amplitude in the in-line direction (A_x/L) as a function of the reduced velocity (V_r) for array of four floating cylinders with circular, square and diamond sections for 0-degree incidence

Figure 9 presents the results of the A_y/L as a function of the V_r for the array of four floating circular, square and diamond cylinders with 0-degree incidence. The results showed that the highest amplitudes occurred for the array of circular cylinders, and the VIV behavior is almost the same of the single circular cylinder. Moreover, the square cylinder with 0-degree incidence showed a linear increase in the amplitude with the increase in the V_r; this behavior is similar to

the galloping phenomenon and is also similar to a single square cylinder. The array of diamond cylinders followed the same behavior of the single diamond cylinder until $V_r = 9$, after that the amplitudes were higher.

Figure 9 also presents a comparison between the present results and the results for SS case characterized by four square columns and pontoons by Gonçalves *et al.* (2015). The comparison showed a high difference of amplitudes; the presence of pontoons had a large influence in the VIM phenomenon and needed to be a source of new studies in the future. Moreover, Liu *et al.* (2016a) presented results for an array of four cylinders with square and diamond sections. The comparison of the results was good for the array of diamond cylinders, the difference between the results could come from the different aspect ratio of the columns.

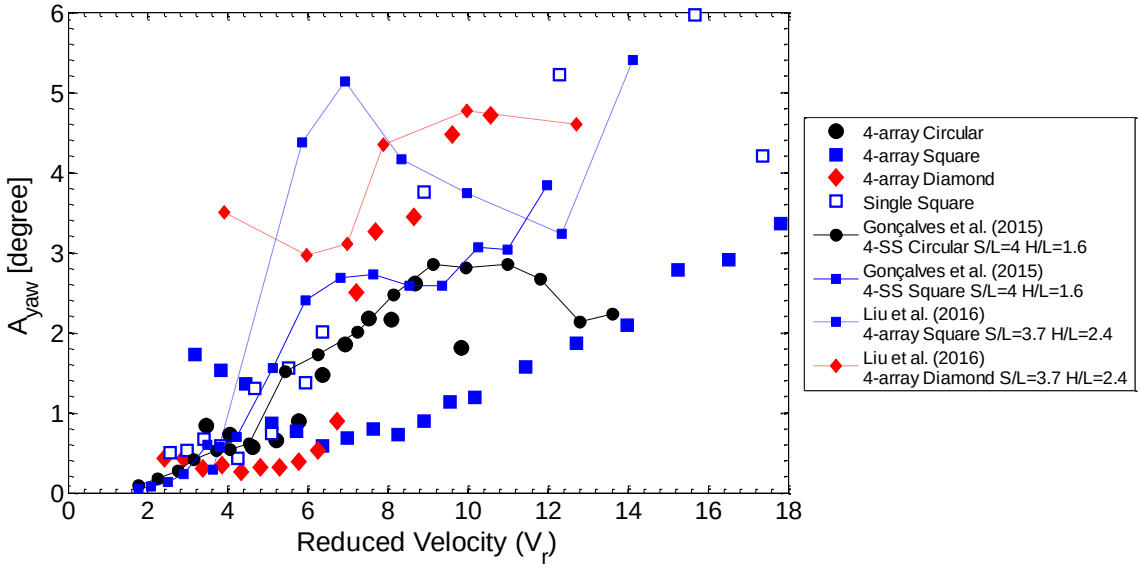

Figure 11: Yaw motion amplitude (A_{yaw}) as a function of the reduced velocity (V_r) for array of four floating cylinders with circular, square and diamond sections for 0-degree incidence

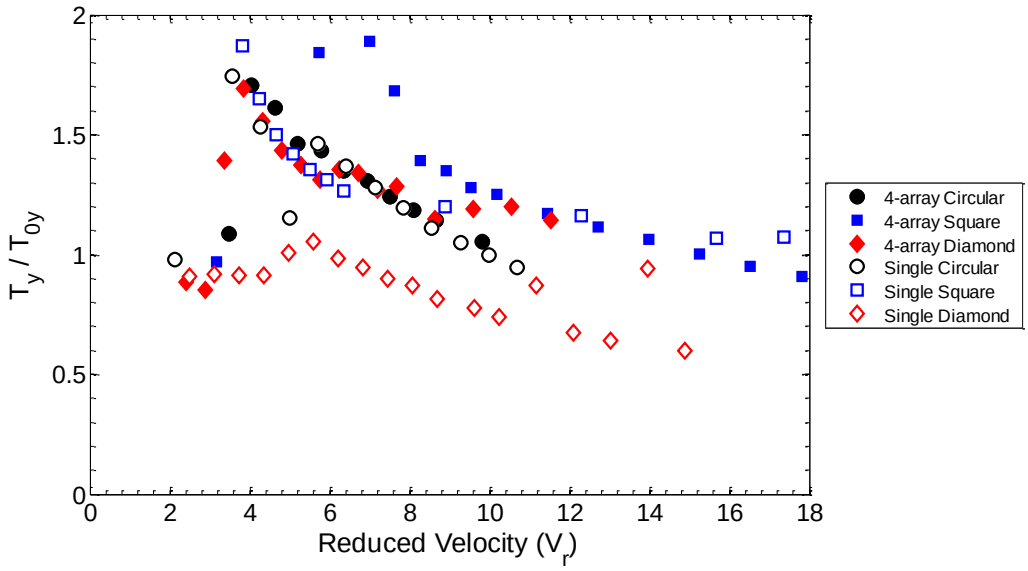

Figure 12: Nondimensional characteristic motion period in the transverse direction (T_y/T_{oy}) as a function of the reduced velocity (V_r) for array of four floating cylinders with circular, square and diamond sections for 0-degree incidence

Figure 10 presents the results of the A_x/L as a function of the V_r for the array of four floating circular, square and diamond cylinders with 0-degree incidence. The results showed the same behavior presented in the transverse direction for the array of circular cylinders. On the other hand, for the array of square cylinders the difference between the array results and the single cylinder was large, and in this case, the results are more similar to the SS case.

Figure 11 presents the results of the A_{yaw} as a function of the V_r for the array of four floating circular, square and diamond cylinders with 0-degree incidence. The results showed a linear increase of the yaw amplitude with the increase of the V_r; this behavior can characterize a galloping phenomenon. On the other hand, the comparison between the array of four cylinders and the SS showed a large difference; thus the pontoon affects a lot the FIM also for yaw motions. The difference between Liu *et al.* (2016a) results and the present results can come from the aspect ratio and distance between columns, mainly for the diamond cases.

Figure 12 presents the results of the T_y/T_{0y} – nondimensional characteristic period as a function of the V_r for the array of four floating circular, square and diamond cylinders with 0-degree incidence. The results showed a similar behavior for the circular cases, i.e., single and array of four cylinders. On the other hand, the values for the array of four cylinders are higher than the single cases. All the results presented the same behavior, a decrease with the increase of the reduced velocity.

3.3 Array of three cylinders

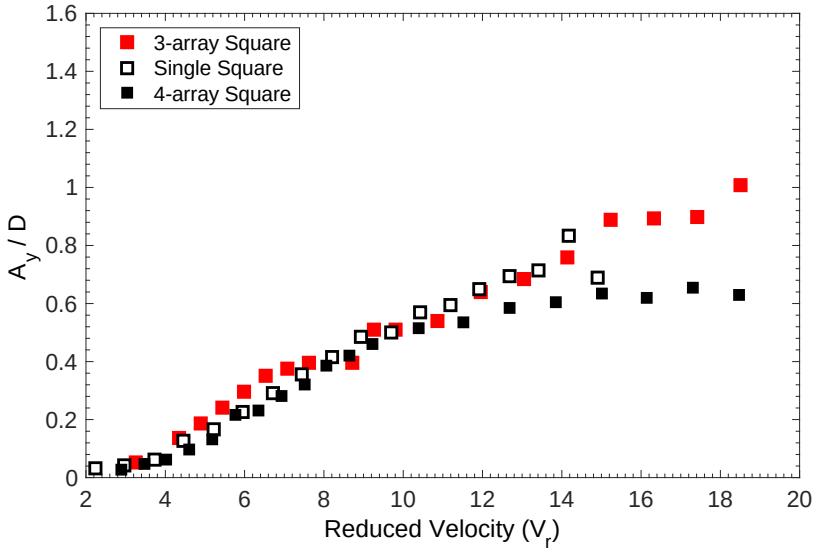

Figure 13: Nondimensional motion amplitude in the transverse direction (A_y/D) as a function of the reduced velocity (V_r) for the single cylinder, the array of three and four floating cylinders with square section for 0-degree incidence and $S/L = 4$

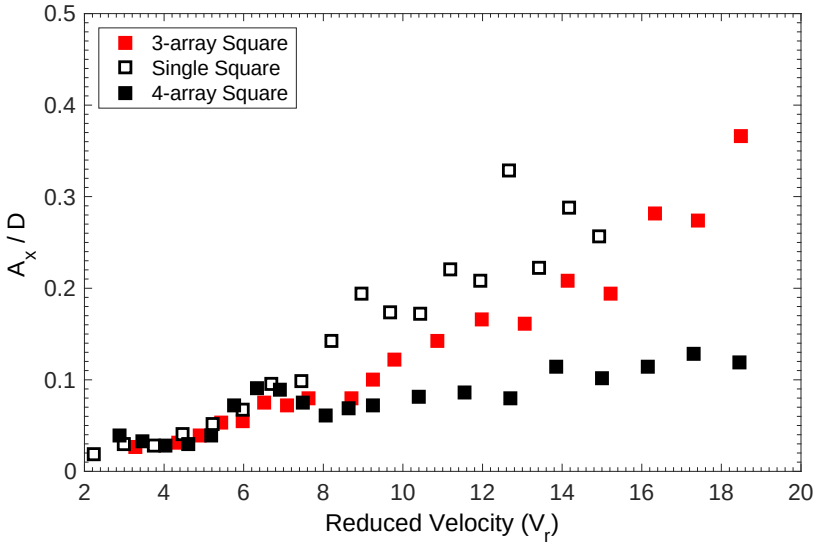

Figure 14: Nondimensional motion amplitude in the in-line direction (A_x/D) as a function of the reduced velocity (V_r) for the single cylinder, the array of three and four floating cylinders with square section for 0-degree incidence and $S/L = 4$

Figure 13 presents the results of the A_y/D as a function of the V_r for the array of three floating square cylinders with 0-degree incidence compared with the results for the single square cylinder and the array of four square cylinders. The results showed that the highest amplitudes in the range $3 < V_r < 8$ occurred for the array of three square cylinders, and the FIM behavior, in this case, is almost the same of the single circular cylinder. Moreover, the array of three cylinders showed a linear increase in the amplitude with the increase in the V_r; this behavior is similar to the galloping phenomenon and is also similar to the single square cylinder. The amplitudes for the array of four cylinders distinguish after $V_r > 10$, smaller amplitudes than the array of three cylinders were observed.

Figure 14 presents the results of the A_x/D as a function of the V_r for the array of three floating square cylinders with 0-degree incidence. In this case, the behavior for all cases is similar up to $V_r = 7$, after this value of reduced velocity the amplitude in the in-line increases linearly for all cases. The amplitudes values for the array of three square columns are between the single square cylinder case and the array of four square cylinders, the highest and lowest amplitudes respectively.

4. CONCLUSIONS

Experiments were performed in a towing tank with an array of circular, square and diamond cylinders. The amplitude results showed a VIV behavior for the single circular cylinder; for the single square cylinder, galloping behavior was observed for 0-degree incidence, and VIV one was observed for 45-degree incidence. The amplitude results for the array of four cylinders were very similar to single cylinders for the distance between cylinders $S/L = 4$. These results are larger than VIM results obtained from a floating system with pontoons. Moreover, the amplitude results for the array of three cylinders were also very similar to single cylinders in the transverse direction and higher than the array of four columns. The amplitudes in the in-line direction showed a larger difference between four and three cylinders. Also, the amplitudes in the in-line direction were higher for the array of three cylinders than for four cylinders one. These results showed the importance to consider the number and geometry of columns for multi-column floaters correctly.

5. ACKNOWLEDGEMENTS

The authors would like to thank JASNAOE – The Japan Society of Naval Architects and Ocean Engineers for the opportunity and support given throughout the project “Brazil-Japan Collaborative Research Program" supporting the internship period of the authors Lopes, P.P.S.P., Hannes, N. and Chame, M.E. during the experiment period in Japan.

6. REFERENCES

Blevins, R.D. and Coughran, C.S., 2009. “Experimental investigation of vortex-induced vibration in one and two dimensions with variable mass, damping, and Reynolds number”. *Journal of Fluids Engineering*, Vol. 131, p. 101202-7.

Fujarra, A.L.C., Rosetti, G.F., Wilde, J. and Gonçalves, R.T., 2012. “State-of-art on vortex-induced motion: A comprehensive survey after more than one decade of experimental investigation”. In *Proceedings of the ASME 2012 31st International Conference on Ocean, Offshore and Arctic Engineering – OMAE2012-83561*. Rio de Janeiro, Brazil.

Gonçalves, R.T., Rosetti, G.F., Fujarra, A.L.C., Franzini, G.R., Freire, C.M. and Meneghini, J.R., 2012. “Experimental comparison of two degrees-of-freedom vortex-induced vibration on high and low aspect ratio cylinders with small mass ratio”. *Journal of Vibration and Acoustics*, Vol. 134, p. 061009-1-7.

Gonçalves, R.T. and Fujarra, A.L.C., 2014. “Experimental study on vortex-induced vibration of floating circular cylinders with low aspect ratio”. In *Proceedings of the ASME 2014 33rd International Conference on Ocean, Offshore and Arctic Engineering – OMAE2014-23383*. San Francisco, CA, USA.

Gonçalves, R.T., Fujarra, A.L.C., Rosetti, G.F., Kogishi, A.M. and Koop A., 2015a. “Effects of column designs on the VIM response of deep-draft semi-submersible platforms”. In *Proceedings of the 25th 2015 International Ocean and Polar Engineering Conference*. Kona, Big Island, Hawaii, USA.

Gonçalves, R.T., Gambarine, D.M., Figueiredo, F.P., Amorim, F.V. and Fujarra, A.L.C., 2015b. “Experimental study on flow-induced vibration of floating squared section cylinders with low aspect ratio, Part I: Effects of incidence angle”. In *Proceedings of the ASME 2015 34th International Conference on Ocean, Offshore and Arctic Engineering – OMAE2015-41008*. St. Johns, NL, Canada.

Gonçalves, R.T., Gambarine, D.M., Momenti, A.M., Figueiredo, F.P. and Fujarra, A.L.C., 2016. “Experimental study on flow-induced vibration of floating squared section cylinders with low aspect ratio, Part II: Effects of rounded edges”. In *Proceedings of the ASME 2016 35th International Conference on Ocean, Offshore and Arctic Engineering, - OMAE2016-54813*. Busan, South Korea.

Liu, M., Xiao, L., Lu, H. and Shi, J., 2016a. “Experimental investigation into the influences of pontoon and column configuration on vortex-induced motions of deep-draft semi-submersibles”. *Ocean Engineering*, Vol. 23, p. 262-277.

Liu, Y., Li, S., Yi, Q. and Chen, D., 2016b. "Developments in semi-submersible floating foundations supporting wind turbines: A comprehensive review", *Renewable and Sustainable Energy Reviews*, Vol. 60, p. 433-449.

Rahman, M.A.A. and Thiagarajan, K., 2013. "Vortex-induced vibration of cylindrical structure with different aspect ratio". In *Proceedings of the 17th International Offshore and Polar Engineering Conference*, Alaska, USA.

Ramirez, M.A.M. and Fernandes, A.C., 2016. "Novel experimental investigation on vortex induced motions of a tension leg platform". In *Proceedings of the ASME 35th International Conference on Ocean, Offshore and Arctic Engineering – OMAE2016-54530*. Busan, South Korea.

Wang, C.M., Utsunomiya, T., Wee, S.C. and Choo, Y.S., 2010. "Research on floating wind turbines: a literature survey". *The IES Journal Part A: Civil & Structural Engineering*, Vol. 3(4), p. 267-277.

Zhao, M. and Cheng, L., 2014. "Vortex-induced vibration of a circular cylinder of finite length". *Physics of Fluid*, Vol. 26, p. 015111-1-26.

Zhao, J., Leontini, J.S., Jacono, D.L. and Sheridan J., 2014. "Fluid–structure interaction of a square cylinder at different angles of attack". *Journal of Fluid Mechanics*, Vol.. 747, p. 688-721.

7. RESPONSIBILITY NOTICE

The authors are the only responsible for the printed material included in this paper.